*Romanian Reports in Physics, Vol. 65, No. 3, P. 688–692, 2013*

*Dedicated to Professor Valentin I. Vlad's 70$^{\text{th}}$ Anniversary*

# A MOLECULAR STATE IN THE $^{14}$C-EMISSION FROM $^{222}$Ra

A. SANDULESCU[1,2], M. MIREA[2,a]

[1]Institute for Advanced Studies in Physics, Romanian Academy, Bucharest, Romania
[2]Horia Hulubei National Institute for Physics and Nuclear Engineering,
PO Box MG-6, Bucharest, Romania
*E-mail*[a]: mirea@nipne.ro

*Received March 25, 2013*

*Abstract.* Shell effects are responsible for the molecular state identified in the cluster emission from $^{222}$Ra. This molecular state was obtained for a mass asymmetry compatible with the $^{14}$C decay. A valley in the external barrier landscape was also evidenced allowing superasymmetric fission. The potential energy was computed in the framework of the macroscopic-microscopic approach based onto the Woods-Saxon two center shell model.

*Key words*: Cluster emission, two-center shell model.

*PACS*: 23.70.+j,24.10.-i

## 1. INTRODUCTION

The heavy ion emission was experimentally evidenced in 1984 [1–4], following earlier theoretical predictions [5–10] obtained within phenomenological models. Several ideas emerge from such treatments that invoke mainly two main ingredients, that is, the external Coulomb barrier and the $Q$-values of the reaction: the internal barrier must be small, the inertia has values close to the reduced mass and the external barrier is mainly given by the Coulomb interaction. Recently, we developed the macroscopic-microscopic approach in order to to treat in a unitary manner the cluster decay, the alpha emission and the cold fission process. A magic valley in the potential energy surface was evidenced [11–15] for cluster and alpha decay. This valley belongs to a mass asymmetry consistent with the formation of a magic daughter and has its origin in the shell effects fluctuations. In the case of cluster decay, the common daughter is the $^{208}$Pb isotope. At the same time, a similar valley was obtained within the Hartree-Fock-Bogoliubov approximation [16, 17]. It is worth to mention that two valleys in the macroscopic-microscopic potential landscape were identified for the first time in Ref. [18]. One of these valleys corresponds to fission, while the

second one, called fusion valley in Ref. [18] is related to a mass asymmetry compatible with the existence of a Pb daughter in a composite system. These two valleys are separated by a ridge. Our investigation of the $^{14}$C emission from $^{222}$Ra shows that this particular reaction is favored by the existence of a molecular state.

## 2. MODEL

In the macroscopic-microscopic approach the behavior of the liquid drop model is mixed within microscopic properties. It is considered that a macroscopic model, as the liquid drop one, describes quantitatively the smooth trends of the potential energy with respect to the particle number and deformation. The microscopic approach determines local fluctuations managed by the shell model. The combined macroscopic-microscopic method is able to reproduce both smooth trends and local fluctuations in the total energy of the nuclear system. In the macroscopic-microscopic method, the nuclear system is forced to deform. The deformations are defined by by some collective coordinates. Each deformation approximately determine all the intrinsic variables. Therefore, the basic ingredient is the shape parametrization. The macroscopic deformation energy is calculated within the liquid drop model. The finite range liquid drop model [19] extended for binary system with different charge densities [20] is used in this paper. The microscopic correction is evaluated within the Strutinsky method [21]. The deformations from one initial nucleus to the separated fragments are obtained by smoothly joining two spheroids of semi-axis $a_i$ and $b_i$ ($i$ = 1,2) with a neck surface generated by the rotation of a circle around the axis of symmetry. By imposing the condition of volume conservation we are left with five independent generalized coordinates $q_j$ ($j$ = 1,5) that can be associated with five degrees of freedom: the elongation $R$ given by the distance between the centers of the spheroids; the necking parameter $C = S/R_3$ related to the curvature of the neck, the eccentricities $\epsilon_i$ associated with the deformations of the nascent fragments and the mass asymmetry parameter $\eta = a_1/a_2$. For the microscopic corrections, a two-center shell model with a Woods-Saxon potential was developed recently [22]. The eigenvalues are obtained by diagonalizing the mean field in the two center shell model basis [23, 24]. The validity of this approach was tested for cluster decay [12, 13], cold fission [25–31] and superheavy element synthesis [11, 39, 40] treated as cold rearrangement processes. Other versions of the two center models, based on Nilsson formalism, were also used in the investigation of binary disintegrations [32–38].

## 3. RESULTS AND DISCUSSION

The deformation energy was calculated by spanning the values in the configuration space that are consistent with cluster decay. The ground state of the parent

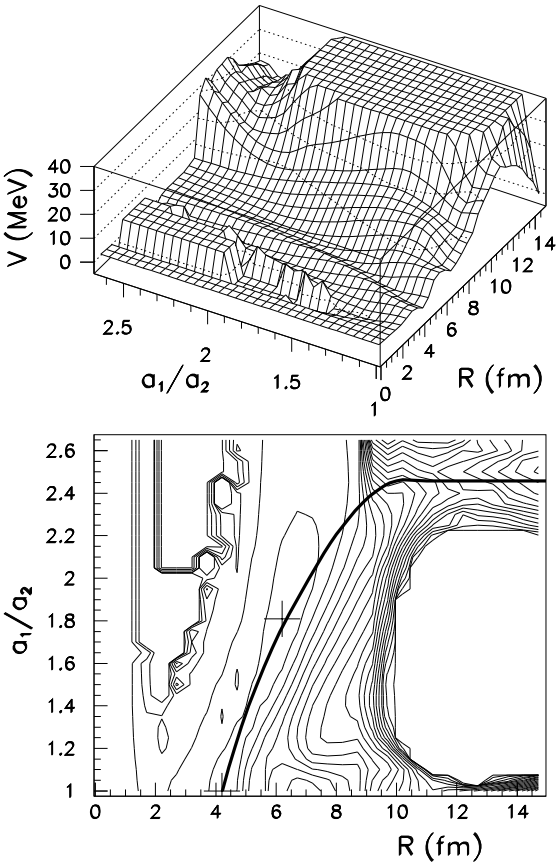


Fig. 1 – The potential energy surface $V$ as function of the elongation $R$ and the mass asymmetry $a_1/a_2$. In the upper panel the potential is represented as a two dimensional histogram. In the lower panel, a contour type representation is used. The step between two equipotential lines is 2 MeV. In the lower panel, the superasymmetric fission trajectory is plotted with a thick line. The ground state and the molecular state are marked with crosses.

$^{222}$Ra was obtained at an elongation $R \approx 4.2$ fm. Several trajectories that start from the ground state and reach the scission configuration given by the system $^{208}$Pb+$^{14}$C were tested and the Gamow factor was evaluated. For this purpose the inertia was computed in the framework of the non-adiabatic cranking model [41, 42]. The path that corresponds to the minimal value of the action integral was retained. This path is plotted in the lower panel of Fig. 1. The deformation energy is displayed as function of the mass asymmetry parameter $a_1/a_2$ and the elongation in Fig. 1. In this figure, the variations as function of $R$ for all the remaining generalized coordinates are those obtained for the path characterized by the minimal action. It can be observed that at

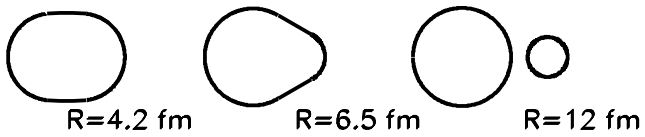


Fig. 2 – Nuclear shapes along the trajectory plotted in Fig. 1. The Shape at $R = 4.2$ is the ground state one. The shape at $R = 6.5$ fm corresponds to the minimum in the molecular state. The shape at $R =$ 12 fm displays the final binary configurations.

$R \approx 6.5$ fm and a mass asymmetry $a_1/a_2 \approx 1.8$, a minimum exists in the potential energy surface. This minimum is marked with a cross and has an energy close to that of the ground state. The energy of this molecular state surpasses that of the ground state with approximately 0.3 MeV. For elongations larger than 9 fm, a valley can be identified in the external barrier. This valley is due to strong negative shell effects of both fragments as evidenced in our previous analysis of the cluster emission [12, 13] and alpha decay [11]. We called in our previous work this valley as a magic valley due to the influence of the magic daughter nucleus.

In Fig. 2, the shapes corresponding to the ground-state, the molecular state and of the asymptotic configuration are plotted. It is evident that the nuclear shape of the molecular state located at approximately $R$=6.5 fm looks like a dinuclear system overlapped. In the molecular state, two distinct fragments separated with an intermediate necked region can be identified.

In the study of the $^{180}$Hg fission, it was evidenced that the local structure of the potential energy landscape is responsible for the mass distribution in fission [31,43]. In the investigated deformation energy of $^{222}$Ra, the molecular minimum favors the $^{14}$C emission and the shell effects of the daughter give rise to a magic valley. The two center model offers the possibility to treat binary emissions like superasymmetric fission processes. This treatment represents an alternative for the preformation models used in $\alpha$-decay [44].

***Acknowledgements.*** Work supported by CNCS-UEFISCDI, project number PN-II-ID-PCE-2011-3-0068.

REFERENCES

1. H.J. Rose and G.A. Jones, Nature **307**, 245 (1984).
2. A. Sandulescu, Yu.S. Zamyatnin, J.A. Lebedev, B.F. Myasoedov, S.P. Tretyakova and D. Hasegan, JINR Rapid Commun. **5**, 5 (1984).
3. S. Gales, E. Hourani , M. Hussonois, H.P. Shapira and M. Vergnes, Phys. Rev. Lett. **53**, 759 (1984).

4. S.W Barwick, P.B. Price and J.D. Stevenson, Phys. Rev. C **31**, 1984 (1984).
5. A. Sandulescu and W. Greiner, J. Phys. G **3**, L189 (1977).
6. A. Sandulescu, H.J. Lustig, J. Hahn and W. Greiner, J. Phys. G **4**, L279 (1978).
7. A. Sandulescu, D.N. Poenaru and W. Greiner, Sov. J. Part. Nucl. **11**, 528 (1980).
8. A. Sandulescu, J. Phys. G **15**, 529 (1989).
9. A. Sandulescu and W. Greiner, Rep. Prog. Phys. **55**, 1423 (1992).
10. A. Sandulescu, D.N. Poenaru, W. Greiner and J.H. Hamilton, Phys. Rev. Lett. **54**, 490 (1985).
11. A. Sandulescu, M. Mirea and D.S. Delion, EPL **101**, 62001 (2013).
12. M. Mirea, A. Sandulescu, and D.S. Delion, Eur. Phys. J. A **48**, 86 (2012).
13. M. Mirea, A. Sandulescu and D.S. Delion, Nucl. Phys. A **870-871**, 23 (2011).
14. M. Mirea, A. Sandulescu and D.S. Delion, Proc. Rom. Acad. Series A **12**, 203 (2011).
15. M. Mirea, Rom. J. Phys. **57**, 372 (2012).
16. M. Warda and L.M. Robledo, Phys. Rev. C **84**, 044608 (2011).
17. M. Warda, Acta Phys. Pol. B **42**, 477 (2011).
18. T. Ichikawa, A. Iwamoto, P. Moller and A.J. Sierk, Phys. Rev. C. **71**, 044608 (2005).
19. P. Moller, J.R. Nix, W.D. Myers and W.J. Swiatecki, Atom. Data Nucl. Data Tabl. **59**, 185 (1995).
20. M. Mirea, O. Bajeat, F. Clapier, F. Ibrahim, A.C. Mueller, N. Pauwels and J. Proust, Eur. Phys. J. A **11**, 59 (2001).
21. M. Brack, J. Damgaard, A. Jensen, H. Pauli, V. Strutinsky and W. Wong, Rev. Mod. Phys. **44**, 320 (1972).
22. M. Mirea, Phys. Rev. C **78**, 044618 (2008).
23. M. Mirea, Phys. Rev. C **54**, 302 (1996).
24. M. Mirea, Nucl. Phys. A **780**, 13 (2006).
25. M. Mirea, Phys. Rev. C **83**, 054608 (2011).
26. M. Mirea, Phys. Lett. B **680**, 316 (2009).
27. M. Mirea, Phys. Lett. B **717** 252 (2012).
28. M. Mirea, D.S. Delion and A. Sandulescu, Phys. Rev. C **81** 044317 (2010).
29. I. Companis, M. Mirea and A. Isbasescu, Rom. J. Phys. **56**, 63 (2011).
30. M. Mirea and L. Tassan-Got, Centr. Europ. J. Phys. **9**, 116 (2011).
31. A.-M. Micu and M. Mirea, Rom. J. Phys. **58**(7-8), 940 (2013).
32. M.S. Shakib, M.F. Rahimi, M.M. Firoozabadi, Rom. Rep. Phys. **65**(2), 401 (2013).
33. M. Mirea, Phys. Rev. C **63**, 034603 (2001) .
34. M. Mirea, Eur. Phys. J. A **4**, 335 (1999).
35. M. Mirea, L. Tassan-Got, C. Stephan, C.O. Bacri and R.C. Bobulescu, Europhys. Lett. **73**, 705 (2006).
36. M. Mirea and F. Clapier, Europhys. Lett. **40**, 509 (1997).
37. M. Mirea, Phys. Rev. C **57**, 2484 (1998).
38. M. Mirea, Mod. Phys. Lett. A **18**, 1809 (2003).
39. M. Mirea, D.S. Delion and A. Sandulescu, EPL **85** 12001 (2009).
40. P. Stoica, Rom. Rep. Phys. **63**, 76 (2011).
41. M. Mirea and R.C. Bobulescu, J. Phys. G **37**, 055106 (2010).
42. M. Mirea, Rom. Rep. Phys. **63**, 676 (2011).
43. P. Moller, J. Randrup and A.J. Sierk, Phys. Rev. C **85**, 024306 (2012).
44. I. Silisteanu and A.I. Budaca, Rom. J. Phys. **57**, 493 (2012).